JAERI-M
93-238

CRITICAL HEAT FLUX FOR ROD BUNDLE UNDER HIGH-PRESSURE BOIL-OFF CONDITIONS

December 1993

Zhongchuan GUO*, Hiroshige KUMAMARU
and Yutaka KUKITA

日本原子力研究所
Japan Atomic Energy Research Institute

JAERI-Mレポートは，日本原子力研究所が不定期に公刊している研究報告書です。
入手の問合わせは，日本原子力研究所技術情報部情報資料課（〒319－11茨城県那珂郡東海村）あて，お申しこしください。なお，このほかに財団法人原子力弘済会資料センター（〒319-11茨城県那珂郡東海村日本原子力研究所内）で複写による実費頒布をおこなっております。

JAERI-M reports are issued irregularly.
Inquiries about availability of the reports should be addressed to Information Division, Department of Technical Information, Japan Atomic Energy Research Institute, Tokai-mura, Naka-gun, Ibaraki-ken 319-11, Japan.

編集兼発行　日本原子力研究所
印　　刷　日立高速印刷株式会社

Critical Heat Flux for Rod Bundle under High-pressure Boil-off Conditions

Zhongchuan GUO*, Hiroshige KUMAMARU and Yutaka KUKITA

Department of Reactor Safety Research
Tokai Research Establishment
Japan Atomic Energy Research Institute
Tokai-mura, Naka-gun, Ibaraki-ken

(Received November 12, 1993)

Critical heat flux (CHF) tests were carried out using a 5 x 5 rod bundle test section of the Two-Phase Flow Test Facility (TPTF). The tests represented high-pressure core inventory boil-off and rod dryout situations which may occur during a small break loss-of-coolant accident (LOCA) or an anticipated transient without scram (ATWS) in a light water reactor. Pressures ranging from 3 to 12 MPa, mass fluxes from 17 to 94 kg/m^2 s and heat fluxes from 3.3 to 18 W/cm^2 were covered. Data were compared with low-flow boiling CHF correlations to examine the applicability of these correlations to high-pressure boil-off. The dryout in the tests occurred at an elevation where the equilibrium quality nearly reached unity.

Keywords : Critical Heat Flux, Boil-off, Dryout, Small Break LOCA, ATWS, Rod Bundle, TPTF.

---

* Nuclear Power Research & Design Institute of China (NPIC), China. Visiting scientist (March 27 - September 26, 1990) under the Science and Technology Agency (STA) Scientist Exchange Program.

高圧ボイルオフ条件下におけるロッドバンドルの限界熱流束

日本原子力研究所東海研究所原子炉安全工学部
郭　忠川*・熊丸　博滋・久木田　豊

(1993年11月12日受理)

小型定常二相流実験装置（TPTF）の5×5ロッドバンドル試験部を用いて，限界熱流束（CHF）実験を実施した。実験は，軽水炉の小破断冷却材喪失事故（LOCA）あるいはスクラム失敗事故（ATWS）時に発生する高圧下の炉心インベントリ　ボイルオフ及び燃料棒ドライアウト状況を模擬して実施した。実験は，圧力：3～12MPa，質量流束：17～94kg／m^2s及び熱流束：3.3～18W／cm^2の範囲をカバーしている。実験データを低流量流動沸騰CHF相関式と比較し，それらの相関式の高圧ボイルオフ条件への適用性を検討した。実験では，ドライアウトは平衡クオリティがほぼ1になった位置において発生した。

東海研究所：〒319－11 茨城県那珂郡東海村白方字白根2－4

＊　中国核動力研究設計院（NPIC）科学技術庁（STA）原子力研究交流制度による受入れ研究員（1990年3月27日～9月26日）

Contents

目　　次

Nomenclature

d:	Diameter (of tube)	m
d_h :	Equivalent diameter	m
d_{he}:	Heated equivalent diameter	m
d_{hy}:	Hydraulic equivalent diameter	m
G :	Mass flux	kg/m^2 s
H_{fg}:	Latent heat of vaporization	J/kg
ΔH_i:	Inlet subcooling enthalpy	J/kg
l :	Heated length	m
l_{bo}:	Boiling length	m
l_{do}:	Dryout point measured from inlet	m
P :	Pressure	Pa
q_c :	Critical heat flux	W/cm^2
q_{cc}:	Critical heat flux calculated by correlation	W/cm^2
q_{ce}:	Critical heat flux, experimental data	W/cm^2
X_{in}:	Inlet quality	
ρ_l :	Density of liquid	kg/m^3
σ :	Surface tension	N/m

A, A_1, A_2, B, C, F_p, F_1, F_2, K, P_T, q_{co} and Y: Refer to Table 2

1. Introduction

For certain classes of accidents* in light water reactors (LWRs), there is the possibility that the core inlet flow rate becomes too small to replenish the core coolant inventory which boils away due to the residual core power. If such uncompensated coolant boil-off should continue, the two-phase mixture level in the vessel will drop, eventually drying out the upper portion of the fuel rod. The dry fuel rod surfaces will heat up, as shown in Fig. 1, endangering the fuel rod integrity. It is, therefore, crucial for reactor safety analyses to predict the occurrence of core dryout as well as the extent of dryout. For low heat fluxes typical of core decay power, the mixture level is clear-cut and dryout occurs immediately above the mixture level as shown in Fig. 1(a). For somehow higher heat fluxes, the dryout front will have an appearance like Fig. 1 (b) with liquid entrainment in the gas phase. In safety-analysis computer codes, the dryout level is predicted by using critical heat flux (CHF) correlations developed from experimental data.

CHF under typical LWR core boil-off conditions has been, however, studied scarcely.[1,2] Tests representing the LWR core geometry have been conducted so far mostly for much higher mass fluxes than the typical values** for boil-off.

This report presents CHF data obtained for high-pressure boil-off conditions using a test section simulating a BWR 8x8 fuel bundle. The data

---

* Such accidents include small-break loss-of-coolant accidents (LOCAs) in a pressurized water reactor (PWR), with the break flow rate too large to be compensated by the high pressure injection (HPI) system, or an anticipated transient without scram (ATWS) in a boiling water reactor (BWR) involving loss of feedwater.

** At the maximum decay power level (6% of the rated power) the core inventory boil-off rate corresponds to a core inlet mass flow of about 18 kg/m^{2}s for a BWR 8x8 bundle and about 30 kg/m^{2}s for PWR 17x17 bundle, at a pressure of 7 MPa. That is, core boil-down at decay power level can occur only if the core inlet flow is smaller than these values. In postulated ATWS situations, the boil-off rates can be greater.

are compared with the Bowring[3] and Katto[4] correlations, and an equation derived from an energy balance assumption (called "V-equation" in this paper)[1] to examine the applicability of these correlations to boil-off conditions.

2. Test Facility

The Two-Phase Flow Test Facility (TPTF)[5] is a separate effect test facility built for the Rig-Of-Safety Assessment Number 4 (ROSA-IV) Program for the study of small-break LOCAs and abnormal transients in pressurized water reactors (PWRs). This facility is now used for the ROSA-V Program for the study of accident management (AM) measures for prevention of severe core damage in PWRs. The primary objective of the TPTF tests is to obtain fundamental data on thermal-hydraulic behavior during accidents in a nuclear reactor: in particular heat transfer in an uncovered core and two-phase flow in horizontal legs. The core heat transfer test section was used for the present high-pressure boil-off tests.

Figure 2 shows the flow diagram of the TPTF. The steam drum produces high-pressure saturated steam and water. For testing in the heat transfer test section, the steam and water in the steam drum are sent separately to the mixer, located beneath the test section, by a steam pump and a water circulation pump, respectively. The steam and water flow rates are adjusted to obtain a desired mixture quality at the outlet of the mixer. The steam-water two-phase mixture then flows into the test section, is heated in the test section, and finally returns to the steam drum.

Figure 3 shows details of a heated rod assembly simulating a BWR 8x8 type fuel assembly. The assembly, installed in a square channel, consists of 25 heated rods with an outer diameter of 12.27 $\pm$0.05 mm and with a heated length of 3.7 m $\pm$37 mm. The heated rods are arranged in a a 5x5 square lattice with a 16.16 $\pm$0.2 mm pitch and supported by upper and lower tie plates and 9 spacers. The hydraulic equivalent diameter d_{hy} is 14.83 mm for the central subchannels. The heated equivalent diameter d_{he} is the same as d_{hy} for the central subchannels where the wetted perimeter equals the heated perimeter. The radial and axial power profiles are uniform.

Figure 4 shows details of the heated rod. The rod axial length consists of three parts: 1.1-m non-heated length at the entrance, 3.7-m

are compared with the Bowring[3] and Katto[4] correlations, and an equation derived from an energy balance assumption (called "V-equation" in this paper)[1] to examine the applicability of these correlations to boil-off conditions.

2. Test Facility

The Two-Phase Flow Test Facility (TPTF)[5] is a separate effect test facility built for the Rig-Of-Safety Assessment Number 4 (ROSA-IV) Program for the study of small-break LOCAs and abnormal transients in pressurized water reactors (PWRs). This facility is now used for the ROSA-V Program for the study of accident management (AM) measures for prevention of severe core damage in PWRs. The primary objective of the TPTF tests is to obtain fundamental data on thermal-hydraulic behavior during accidents in a nuclear reactor: in particular heat transfer in an uncovered core and two-phase flow in horizontal legs. The core heat transfer test section was used for the present high-pressure boil-off tests.

Figure 2 shows the flow diagram of the TPTF. The steam drum produces high-pressure saturated steam and water. For testing in the heat transfer test section, the steam and water in the steam drum are sent separately to the mixer, located beneath the test section, by a steam pump and a water circulation pump, respectively. The steam and water flow rates are adjusted to obtain a desired mixture quality at the outlet of the mixer. The steam-water two-phase mixture then flows into the test section, is heated in the test section, and finally returns to the steam drum.

Figure 3 shows details of a heated rod assembly simulating a BWR 8x8 type fuel assembly. The assembly, installed in a square channel, consists of 25 heated rods with an outer diameter of 12.27 $\pm$0.05 mm and with a heated length of 3.7 m $\pm$37 mm. The heated rods are arranged in a a 5x5 square lattice with a 16.16 $\pm$0.2 mm pitch and supported by upper and lower tie plates and 9 spacers. The hydraulic equivalent diameter d_{hy} is 14.83 mm for the central subchannels. The heated equivalent diameter d_{he} is the same as d_{hy} for the central subchannels where the wetted perimeter equals the heated perimeter. The radial and axial power profiles are uniform.

Figure 4 shows details of the heated rod. The rod axial length consists of three parts: 1.1-m non-heated length at the entrance, 3.7-m

heated length and 0.13-m non-heated length at the outlet. The sheath and the heater element are made of Inconel 600 and Nichrome-5, respectively. The electric insulator inside the heater element is sintered boron nitride (BN) and the insulator between the heater element and the sheath is packed BN.

Ninety-nine (99) Chromel-Alumel (C/A) thermocouples with an outer diameter (OD) of 0.5 mm, embedded on the outer surfaces of 9 heater rods (Rod Nos. 1, 7, 8, 11, 12, 13, 15, 19 and 25), measure the rod surface temperatures. The azimuthal orientations and the 11 axial locations of the thermocouples are shown in Fig. 3. Forty (40) 0.65-mm OD thermocouples, installed just upstream of the spacers, measure the fluid temperatures. Ten (10) 1.6-mm OD thermocouples measure the channel box inner surface temperatures. Twenty-four (24) conductivity probes, installed on the inner surface of the channel box, measure the steam-water mixture levels by detecting the presence of water or steam.

The steam and water flow rates are measured by using orifice flowmeters located upstream the mixer. The pressure and temperature of the mixed fluid are measured at the test section inlet. The power to the heated rod assembly is controlled by a silicon controlled rectifier (SCR) power control system. The heat flux on heated rod surface is calculated from the electric power input to the fuel assembly.

The standard-deviation uncertainties for the measurements are 0.6, 0.6, 0.6 and 1.4% for the pressure, water flow rate, steam flow rate and heat flux respectively, and 4 K and 3 K for the fluid temperatures and the heater rod surface temperatures, respectively.

3. Test Procedure and Test Conditions

3.1 Test procedure

The tests were conducted by supplying nearly saturated water to the test section. After a desired, constant flow rate was reached, power was applied to the bundle. Then the two-phase mixture in the bundle boiled down to the height where the inlet water flow rate balanced with the boil-off rate. The bundle power was controlled so that the maximum heater rod surface temperature was kept at approximately 923 K (650 C). After this steady-state boil-off condition had been reached, data were recorded.

The dryout level was defined, for each heated rod, as the arithmetic

heated length and 0.13-m non-heated length at the outlet. The sheath and the heater element are made of Inconel 600 and Nichrome-5, respectively. The electric insulator inside the heater element is sintered boron nitride (BN) and the insulator between the heater element and the sheath is packed BN.

Ninety-nine (99) Chromel-Alumel (C/A) thermocouples with an outer diameter (OD) of 0.5 mm, embedded on the outer surfaces of 9 heater rods (Rod Nos. 1, 7, 8, 11, 12, 13, 15, 19 and 25), measure the rod surface temperatures. The azimuthal orientations and the 11 axial locations of the thermocouples are shown in Fig. 3. Forty (40) 0.65-mm OD thermocouples, installed just upstream of the spacers, measure the fluid temperatures. Ten (10) 1.6-mm OD thermocouples measure the channel box inner surface temperatures. Twenty-four (24) conductivity probes, installed on the inner surface of the channel box, measure the steam-water mixture levels by detecting the presence of water or steam.

The steam and water flow rates are measured by using orifice flowmeters located upstream the mixer. The pressure and temperature of the mixed fluid are measured at the test section inlet. The power to the heated rod assembly is controlled by a silicon controlled rectifier (SCR) power control system. The heat flux on heated rod surface is calculated from the electric power input to the fuel assembly.

The standard-deviation uncertainties for the measurements are 0.6, 0.6, 0.6 and 1.4% for the pressure, water flow rate, steam flow rate and heat flux respectively, and 4 K and 3 K for the fluid temperatures and the heater rod surface temperatures, respectively.

3. Test Procedure and Test Conditions

3.1 Test procedure

The tests were conducted by supplying nearly saturated water to the test section. After a desired, constant flow rate was reached, power was applied to the bundle. Then the two-phase mixture in the bundle boiled down to the height where the inlet water flow rate balanced with the boil-off rate. The bundle power was controlled so that the maximum heater rod surface temperature was kept at approximately 923 K (650 C). After this steady-state boil-off condition had been reached, data were recorded.

The dryout level was defined, for each heated rod, as the arithmetic

mean level of the lowest thermocouple level, where the measured rod surface temperature exceeded the fluid saturation temperature by more than 20 K, and the adjacent upstream thermocouple level. This procedure allowed the dryout level to be defined with an accuracy of ±17 cm.

The heated rods next to the channel box wall are termed "peripheral" rods and other rods are termed "central" rods in this report. The dryout level averaged over the five instrumented central heated rods, $l_{do(ctr)}$, the level averaged over the four instrumented peripheral heater rods $l_{do(per)}$, and the average over all nine instrumented heater rods $l_{do(avg)}$, were defined for each experiment.

The influence of the choice of equivalent diameters on the performance of correlation is also discussed in Sec. 4.6. In this paper, the equivalent diameters for the central subchannel, the corner subchannel and the whole bundle, as illustrated in Fig. 5, are denoted by $d_{h(ctr)}$, $d_{h(per)}$ and $d_{h(avg)}$, respectively. The corner subchannel was selected as an extreme case for the peripheral region.

3.2 Test Conditions

The tests covered pressures ranging from 3 to 12 MPa, mass fluxes from 17 to 94 kg/m^2 s and heat fluxes from 3.3 to 18 W/cm^2. The test conditions are listed in Table 1.

4. Test Results and Discussions

4.1 Test Results

Eighteen (18) data points were obtained for three different pressures and various mass fluxes. One data point consists of the measured dryout level, heat flux (i.e., CHF), mass flux, inlet subcooling and pressure. It is noted that the dryout level is almost even for most cases.

Four (4) data out of 18 data, Tests 33, 310, 61 and 91 in Table 1, obtained for mass fluxes less than approximately 30 kg/m^{2}s, showed systematic shift from other data as shown in Figs. 6 through 12 presented later. These data mean that dryout occurred at equilibrium qualities less than unity whereas it is unlikely that thermal nonequilibrium at the dryout point becomes more significant with decrease in flow rate. It is likely, rather, that these low-flow tests were affected by the

mean level of the lowest thermocouple level, where the measured rod surface temperature exceeded the fluid saturation temperature by more than 20 K, and the adjacent upstream thermocouple level. This procedure allowed the dryout level to be defined with an accuracy of ±17 cm.

The heated rods next to the channel box wall are termed "peripheral" rods and other rods are termed "central" rods in this report. The dryout level averaged over the five instrumented central heated rods, $l_{do(ctr)}$, the level averaged over the four instrumented peripheral heater rods $l_{do(per)}$, and the average over all nine instrumented heater rods $l_{do(avg)}$, were defined for each experiment.

The influence of the choice of equivalent diameters on the performance of correlation is also discussed in Sec. 4.6. In this paper, the equivalent diameters for the central subchannel, the corner subchannel and the whole bundle, as illustrated in Fig. 5, are denoted by $d_{h(ctr)}$, $d_{h(per)}$ and $d_{h(avg)}$, respectively. The corner subchannel was selected as an extreme case for the peripheral region.

3.2 Test Conditions

The tests covered pressures ranging from 3 to 12 MPa, mass fluxes from 17 to 94 kg/m^2 s and heat fluxes from 3.3 to 18 W/cm^2. The test conditions are listed in Table 1.

4. Test Results and Discussions

4.1 Test Results

Eighteen (18) data points were obtained for three different pressures and various mass fluxes. One data point consists of the measured dryout level, heat flux (i.e., CHF), mass flux, inlet subcooling and pressure. It is noted that the dryout level is almost even for most cases.

Four (4) data out of 18 data, Tests 33, 310, 61 and 91 in Table 1, obtained for mass fluxes less than approximately 30 kg/m^{2}s, showed systematic shift from other data as shown in Figs. 6 through 12 presented later. These data mean that dryout occurred at equilibrium qualities less than unity whereas it is unlikely that thermal nonequilibrium at the dryout point becomes more significant with decrease in flow rate. It is likely, rather, that these low-flow tests were affected by the

experimental uncertainty in the bundle flow rate. Although the measurement of the test section inlet flow rate was accurate, the bundle flow rate was possibly affected by the flow into the annular section surrounding the bundle channel box. This annular section is closed at its top and therefore does not affect the bundle flow rate if a perfect steady state is reached. However, if not, this section communicates with the bundle inlet and can affect the flow rate into the bundle, in particular when the flow rate is small. Therefore, these data are presented with parentheses in Table 1 and also in Figs. 6 through 12. These data are also excluded in the following discussions.

4.2 Available Correlations

In safety-analysis computer codes, the dryout level is predicted by using CHF correlations, or combinations of CHF correlation and void fraction criteria. An example of the latter is the modified Zuber correlation used in the RELAP5/MOD2 code[6].

The present data were compared with three low-flow CHF correlations: the Bowring correlation[3], Katto correlation[4] and the "V-equation"[1], summarized in Table 2.

The Bowring correlation scheme was developed from rod bundle data covering pressures ranging from 0.6 to 15.5 MPa and mass fluxes from 50 to 4000 kg/m^2s. It is a set of correlations which are applicable to specific test section geometries, inlet conditions and so on. The correlation used in the present comparison is the one recommended for the core geometries of pressure-tube reactor, BWR and PWR under subcooled inlet conditions.

The Katto correlation scheme was developed from tube data covering pressures ranging from 2.6 to 20 MPa, mass fluxes from 750 to 4000 kg/m^2s and inlet subcoolings from 0 to 931 kJ/kg. It consists of four separate correlations, each covering different ranges of parameters. According to the criterion given in the scheme, all the present data fall in only one of the four regimes, i.e. the "L-regime" (low-flow regime).

The V-equation is equivalent to the assumption that dryout occurs upon complete evaporation of liquid, i.e., at an axial location where the equilibrium quality reaches unity. The equation can be written in the form shown in Table 2.

4.3 Comparison of Data with Correlations

The following comparisons between the correlations and data are presented in terms of the ratio between the predicted and measured CHFs versus the mass flux. In these comparisons, the equivalent diameter and dryout level are those defined for the central subchannels and central rods, respectively (i.e. $d_{he(ctr)} = d_{hy(ctr)}$, and $l_{do(ctr)}$).

Comparison for the Bowring correlation is shown in Fig. 6. The correlation performs fairly well, particularly for the higher mass fluxes, since the correlation was developed from bundle data covering mass fluxes down to 50 kg/m^2s.

The comparison for the Katto correlation, shown in Fig. 7, is also favorable, although the correlation is based on tube data covering mass fluxes only down to 750 kg/m^2s. For very-low flow rates, the correlation nearly agrees to the V-equation, which predicts the present data within 15% as shown in Fig. 8.

Figure 8 shows that the V-equation also predicts fairly well the present dryout data. This means that the dryout occurs at equilibrium qualities nearly equal to unity. This point will be discussed again in Sec. 4.5.

4.4 Dryout Level Unevenness

It has been reported in literature [7] that dryout occurs at lower elevations in the bundle peripheral region than in the central region since the flow velocity tends to be lower in the former. This is called the "cold wall effect." In the present experiments, however, the dryout level was almost even over the bundle crosssection, as indicated in Table 1, except for higher mass fluxes where the level tended to be lower in the peripheral region.

The differences in the dryout level affected only little the data-correlation comparisons. Figures 9 and 10 show the comparisons for the V-equation where the bundle-average dryout level $l_{do(avg)}$ and the peripheral-rods dryout level $l_{do(per)}$ were used instead of the central-rods dryout level $l_{do(ctr)}$. The equivalent diameter used here is that for the central subchannel, $d_{h(ctr)}$.

4.5 Selection of equivalent diameter

In this report, the experimental data have been compared with correlations where the equivalent diameters were those defined for the central subchannels. Figures 11 and 12 show the comparison results for the V-equation which used equivalent diameters for the whole bundle $d_{h(avg)}$ and corner subchannel $d_{h(per)}$. (In these comparisons, Figs. 11 and 12, $l_{do(ctr)}$ was used for l_{do}.) The comparisons indicate that the equivalent diameter for the whole bundle, $d_{h(avg)}$, is the best choice. This implies that the rod dryout is dictated by the bundle-averaged energy balance rather than the local energy balance for the central subchannels. The bundle-average equilibrium qualities calculated (using $d_{h(avg)}$) for the central-rods dryout level ($l_{do(ctr)}$) are presented in Table 1. The calculated values are close to unity.

5. Conclusions

CHF tests were carried out using a 5 x 5 rod bundle at the TPTF under high-pressure boil-off conditions which are important in the core thermal-hydraulic behavior during a small-break LOCA or an ATWS of a nuclear reactor. Total 18 sets of steady-state CHF data, covering 3 to 12 MPa in pressure, 17 to 94 kg/m^{2}s in mass flux and 3.3 to 18 W/cm^2 in heat flux were obtained. These were compared with the Bowring and Katto correlations as well as the V-equation which assumes that the dryout occurs at an equilibrium quality of unity. The results are summarized as follows.

(1) The above three correlations predicted fairly well the present CHF data.
(2) The dryout level was almost uniform over the bundle cross section, in particular at lower mass fluxes.
(3) The dryout occurred at equilibrium qualities close to unity.

4.5 Selection of equivalent diameter

In this report, the experimental data have been compared with correlations where the equivalent diameters were those defined for the central subchannels. Figures 11 and 12 show the comparison results for the V-equation which used equivalent diameters for the whole bundle $d_{h(avg)}$ and corner subchannel $d_{h(per)}$. (In these comparisons, Figs. 11 and 12, $l_{do(ctr)}$ was used for l_{do}.) The comparisons indicate that the equivalent diameter for the whole bundle, $d_{h(avg)}$, is the best choice. This implies that the rod dryout is dictated by the bundle-averaged energy balance rather than the local energy balance for the central subchannels. The bundle-average equilibrium qualities calculated (using $d_{h(avg)}$) for the central-rods dryout level ($l_{do(ctr)}$) are presented in Table 1. The calculated values are close to unity.

5. Conclusions

CHF tests were carried out using a 5 x 5 rod bundle at the TPTF under high-pressure boil-off conditions which are important in the core thermal-hydraulic behavior during a small-break LOCA or an ATWS of a nuclear reactor. Total 18 sets of steady-state CHF data, covering 3 to 12 MPa in pressure, 17 to 94 kg/m^{2}s in mass flux and 3.3 to 18 W/cm^2 in heat flux were obtained. These were compared with the Bowring and Katto correlations as well as the V-equation which assumes that the dryout occurs at an equilibrium quality of unity. The results are summarized as follows.

(1) The above three correlations predicted fairly well the present CHF data.
(2) The dryout level was almost uniform over the bundle cross section, in particular at lower mass fluxes.
(3) The dryout occurred at equilibrium qualities close to unity.

Acknowledgment

The authors are indebted to their colleagues at the JAERI Thermohydraulic Safety Engineering Laboratory for their valuable suggestions and discussions. Special thanks are due to Mr. H. Murata of JAERI and Mr. H. Yamada and other members of Nuclear Engineering Co. for conducting the tests, Mr. T. Nakajima of ISL Co. for processing the data, and Miss T. Kurosawa of Nihon Computer Bureau for typing the manuscript.

References

[1] Kumamaru, H., Koizumi, Y. and Tasaka, K.: Critical heat flux for uniformly heated rod bundle under high-pressure, low-flow and mixed inlet conditions, J. Nucl. Sci. Technol., 26, 544-557 (1989).

[2] Yoder, G. L., et al.: Rod bundle burnout data and correlation comparisons, Nucl. Technol., 68, 355-369 (1985).

[3] Bowring, R. W.: A new mixed flow cluster dryout correlation for pressures in the range 0.6-15.5 MN/m^2 (90-2,250 psia) - for use in a transient blowdown code, "Heat and Fluid Flow in Water Reactor Safety", p. 175 (1977), Inst. Mech. Engrs.

[4] Katto, Y.: A generalized correlation of critical heat flux for the forced convection boiling in vertical uniformly heated round tubes, Int. J. Heat Mass Transfer, 21, 1527-1542 (1978).

[5] Nakamura, H., et al.: System description for ROSA-IV two-phase flow test facility (TPTF), JAERI-M 83-042, (1983).

[6] Ransom, V. H., et al.: RELAP5/MOD2 code manual, Vol. 1; Code structure, systems models and solution methods, NUREG/CR-4312, EGG-2396, (1985).

[7] Reddy, D. G. and Fighetti, C. F.: Parametric study of CHF data, Vol. 2; A generalized subchannel CHF correlation for PWR and BWR fuel assemblies, EPRI-NP-2609, (1983).

Acknowledgment

The authors are indebted to their colleagues at the JAERI Thermohydraulic Safety Engineering Laboratory for their valuable suggestions and discussions. Special thanks are due to Mr. H. Murata of JAERI and Mr. H. Yamada and other members of Nuclear Engineering Co. for conducting the tests, Mr. T. Nakajima of ISL Co. for processing the data, and Miss T. Kurosawa of Nihon Computer Bureau for typing the manuscript.

References

[1] Kumamaru, H., Koizumi, Y. and Tasaka, K.: Critical heat flux for uniformly heated rod bundle under high-pressure, low-flow and mixed inlet conditions, J. Nucl. Sci. Technol., 26, 544-557 (1989).

[2] Yoder, G. L., et al.: Rod bundle burnout data and correlation comparisons, Nucl. Technol., 68, 355-369 (1985).

[3] Bowring, R. W.: A new mixed flow cluster dryout correlation for pressures in the range 0.6-15.5 MN/m^2 (90-2,250 psia) - for use in a transient blowdown code, "Heat and Fluid Flow in Water Reactor Safety", p. 175 (1977), Inst. Mech. Engrs.

[4] Katto, Y.: A generalized correlation of critical heat flux for the forced convection boiling in vertical uniformly heated round tubes, Int. J. Heat Mass Transfer, 21, 1527-1542 (1978).

[5] Nakamura, H., et al.: System description for ROSA-IV two-phase flow test facility (TPTF), JAERI-M 83-042, (1983).

[6] Ransom, V. H., et al.: RELAP5/MOD2 code manual, Vol. 1; Code structure, systems models and solution methods, NUREG/CR-4312, EGG-2396, (1985).

[7] Reddy, D. G. and Fighetti, C. F.: Parametric study of CHF data, Vol. 2; A generalized subchannel CHF correlation for PWR and BWR fuel assemblies, EPRI-NP-2609, (1983).

Table 1 Test conditions

Test No.	Pressure (MPa)	Mass Flux (kg/m^2s)	Heat Flux (W/cm^2)	Inlet Temp. (K)	Dryout Point (m)			Dryout Quality* (-)
					$l_{do(avg)}$	$l_{do(ctr)}$	$l_{do(per)}$	
(33	3.125	17.039	3.265	475.6	3.049	3.049	3.049	0.6927)
(310	3.427	30.110	5.869	493.2	3.314	3.314	3.314)	0.8172)
321	3.422	39.027	9.102	495.9	3.049	3.049	3.049	0.9127
330	3.412	48.784	11.826	495.4	3.167	3.314	2.983	0.9882
340	3.407	58.062	13.771	497.0	3.137	3.208	3.049	0.9607
30	3.198	66.450	14.658	492.9	3.368	3.622	3.049	0.9488
(61	7.022	20.798	4.007	528.3	2.785	2.785	2.785	0.7448)
612	7.335	36.830	7.378	541.9	3.314	3.314	3.314	0.9941
620	7.329	49.550	10.665	543.8	3.049	3.049	3.049	0.9881
630	7.310	61.908	13.122	541.8	3.020	3.049	2.983	0.9558
640	7.328	75.328	15.852	548.5	3.049	3.102	2.983	0.9828
60	7.139	87.482	18.016	541.2	3.108	3.314	2.851	0.9514
(91	11.875	26.799	4.653	565.8	2.550	2.521	2.587	0.7230)
910	12.216	41.772	7.243	582.7	2.785	2.785	2.785	0.8880
920	12.223	54.782	10.638	580.9	2.521	2.521	2.521	0.8918
930	12.224	67.334	12.933	582.0	2.785	2.785	2.785	0.9879
940	12.216	80.419	15.501	588.4	2.756	2.785	2.719	1.017
90	11.873	93.640	17.034	576.8	2.726	2.785	2.653	0.8810

* Calculated using $d_{h(avg)}$ for $l_{do(ctr)}$.

Table 2 Correlations

Correlation	Equation	Data base range
Bowring	For Subcooled Inlet Condition $q_c = \frac{A+B\Delta H_i}{C+lY}$ $P \leq 1250$ $A = \frac{242.4F_1Gd_{he}}{1+\frac{1.52(F_Pd_{he})^2G}{F_2d_{hy}^{1.3}\{1+G(0.8F_pd_{he}/d_{hy}-1)\}}}$ $B = 0.25Gd_{he} \times \exp(-0.2G)$ $C = 60d_{hy}^{0.57}G^{0.27}(1+\frac{Y-1}{G+1})$ $F_1 = [1.0-0.04P_T(1+0.47P_T^2)^{1/2}]^2$ $F_2 = 0.45 + 1.25P_T$: $P \leq 415$ $= 0.424+1.959P_T-1.556P_T^2$: $415<P\leq650$ $= (3.2-P_T)(0.32+0.135P_T)$: $650<P$ $P_T = 0.001P$ $1250 < P$ $A = A_2 + (2.250-0.001P)(A_1-A_2)$ $A_1 = A$ for $P\leq1250$ with $F_1=0.8726$ and $F_2=0.953$ $A_2 = 18.0G + \frac{9.5Gd_{he}}{0.1+G}$ $B = B$ for $P \leq 1250$ $C = C$ for $P \leq 1250$ $Y = 1$ for uniform axial heat flux distribution $F_P = 1$ for R.P.F. (radial peaking factor) = 1 (Note) $l = l_{do}$ for this study	P: 0.6 - 15.5 MPa G: 50 - 4000 kg/m^2·s Unit q_c : MBtu/ft^{2}h d_{he}: in d_{hy}: in l : in H_{fg}: Btu/lb ΔH_i: Btu/lb P : psia G : Mlb/ft^{2}h

Table 2 Correlations (Continued)

Correlation	Equation	Data base range
Katto	$q_c = q_{co}\{1+K(\Delta H_i/H_{fg})\}$ For L-Regime $\frac{q_{co}}{GH_{fg}} = C\left(\frac{\sigma\rho_l}{G^2 l}\right)^{0.043} \Big/ \left(\frac{l}{d}\right)$ $K = \frac{1.043}{4C(\sigma\rho_l/G^2 l)^{0.043}}$ $C = 0.25$: $l/d<50$ $= 0.34$: $150<l/d$ $= 0.25+0.0009(l/d-50)$: $50<l/d<150$ (Note) $l = l_{do}$ for this study	P: 2.6 - 20 MPa G: 750 - 4000 kg/m^2·s ΔH_i: 0 - 931 kJ/kg
V-equation (Complete vaporization of liquid)	$\frac{q_c}{G(H_{fg}+\Delta H_i)} = \frac{0.25}{l_{do}/d_{he}}$ or $\frac{q_c}{GH_{fg}} = \frac{0.25}{l_{bo}/d_{he}}$	P: 3 - 12 MPa G: 20 - 410 kg/m^2·s X_{in}: 0.4 - 0.9

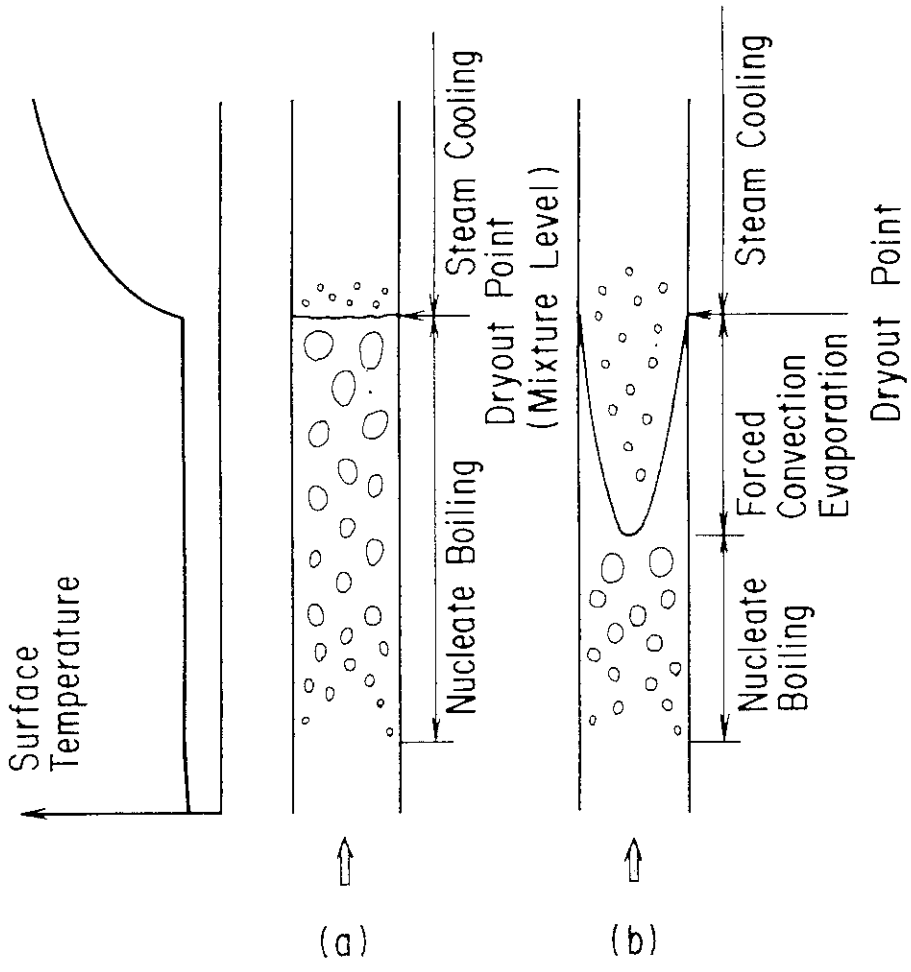

Fig. 1 Schematics of core subchannel flow under boil-off conditions

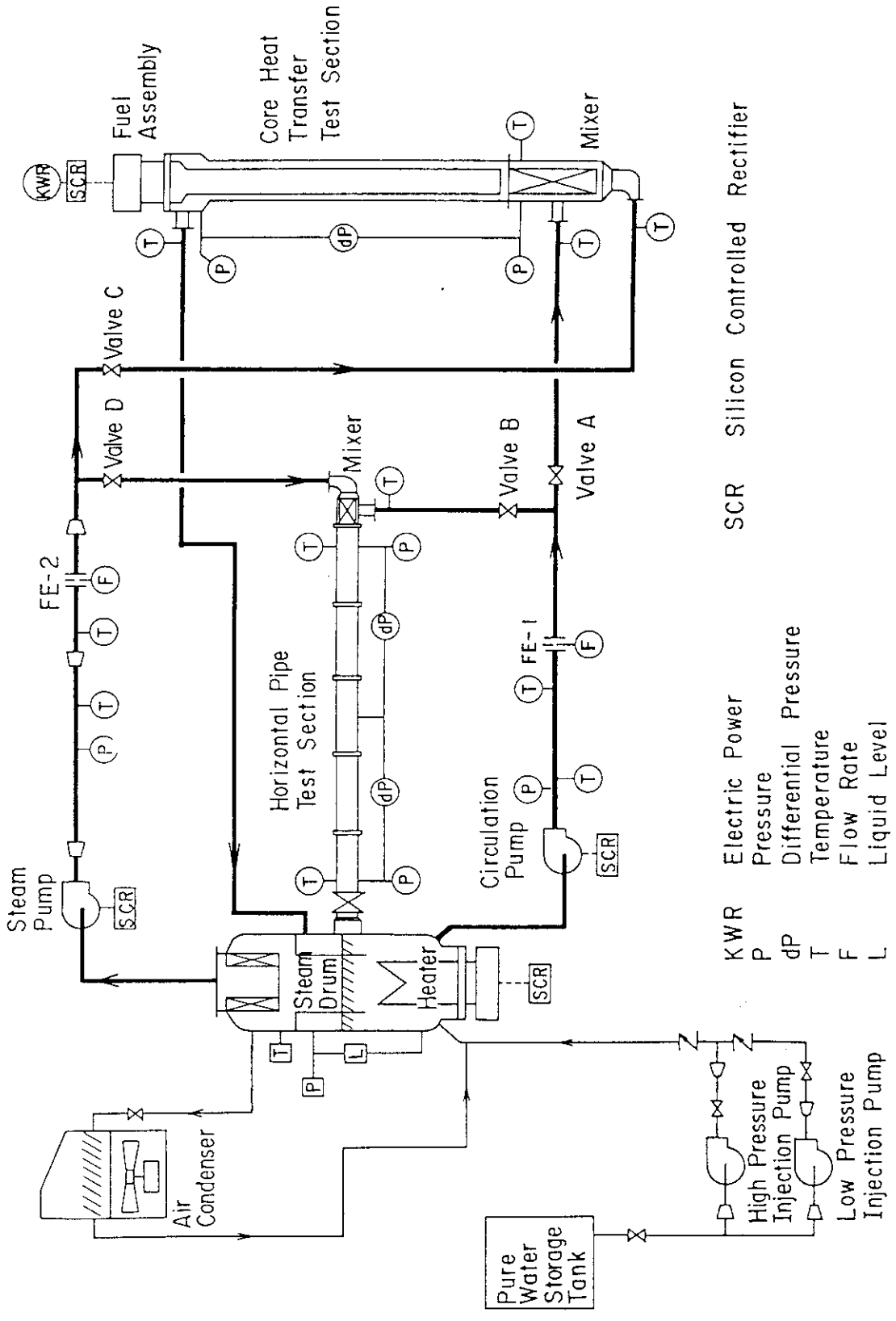

Fig. 2 Flow diagram of TPTF

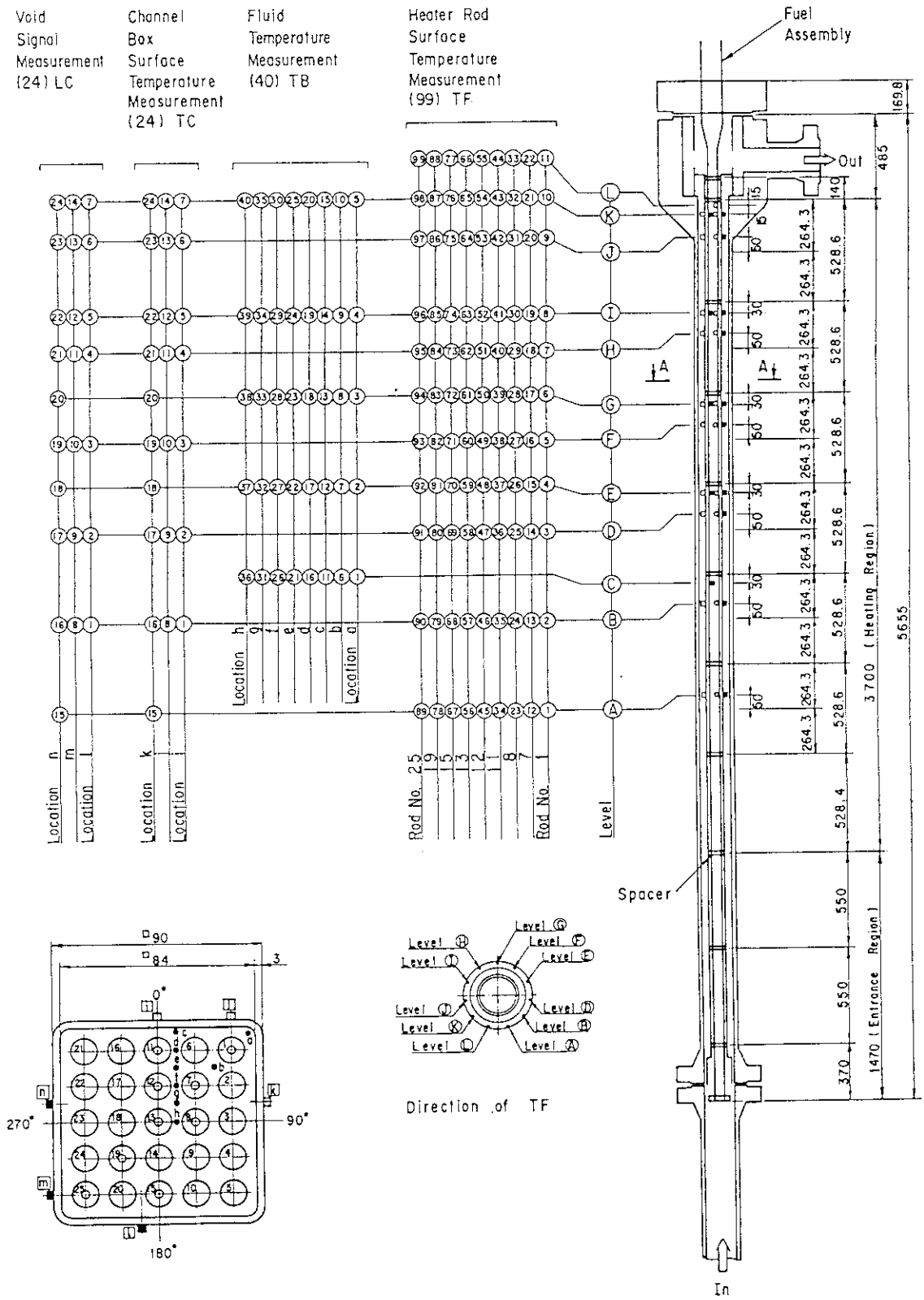

Location of Thermocouple and Void Sensor (A-A Cross Section)

- ○ Heater Rod Surface Temp. TF 11 x 9 = 99
- ● Fluid Temp. TB 8 x 5 = 40
- □ Channel Box Surface Temp. TC 7 x 2 + 10 x 1 = 24
- ■ Void Sensor LC 7 x 2 + 10 x 1 = 24

Fig. 3 Core heat transfer test section

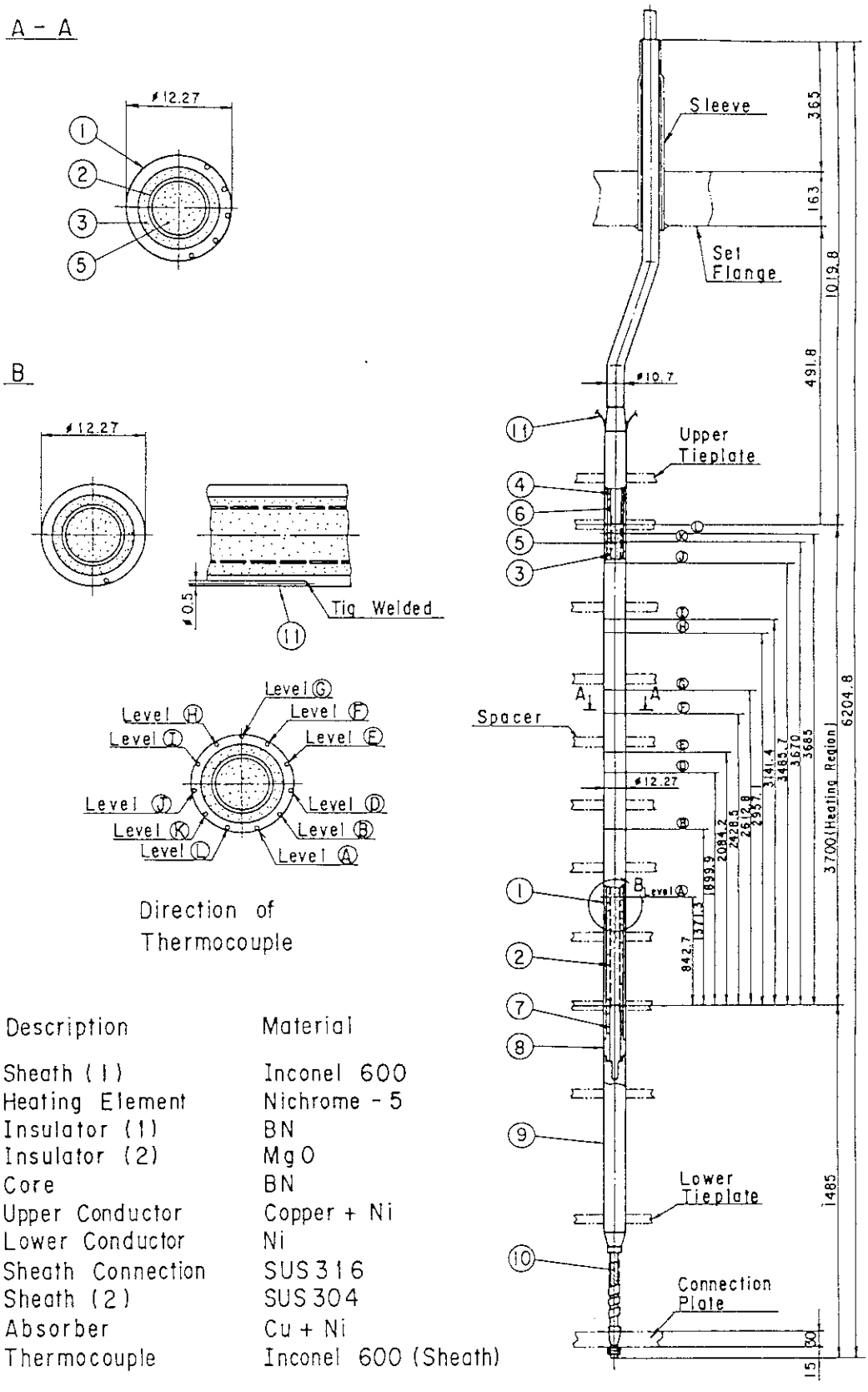

Mark	Description	Material
1	Sheath (1)	Inconel 600
2	Heating Element	Nichrome - 5
3	Insulator (1)	BN
4	Insulator (2)	MgO
5	Core	BN
6	Upper Conductor	Copper + Ni
7	Lower Conductor	Ni
8	Sheath Connection	SUS316
9	Sheath (2)	SUS304
10	Absorber	Cu + Ni
11	Thermocouple	Inconel 600 (Sheath)

Fig. 4 Details of heated rod

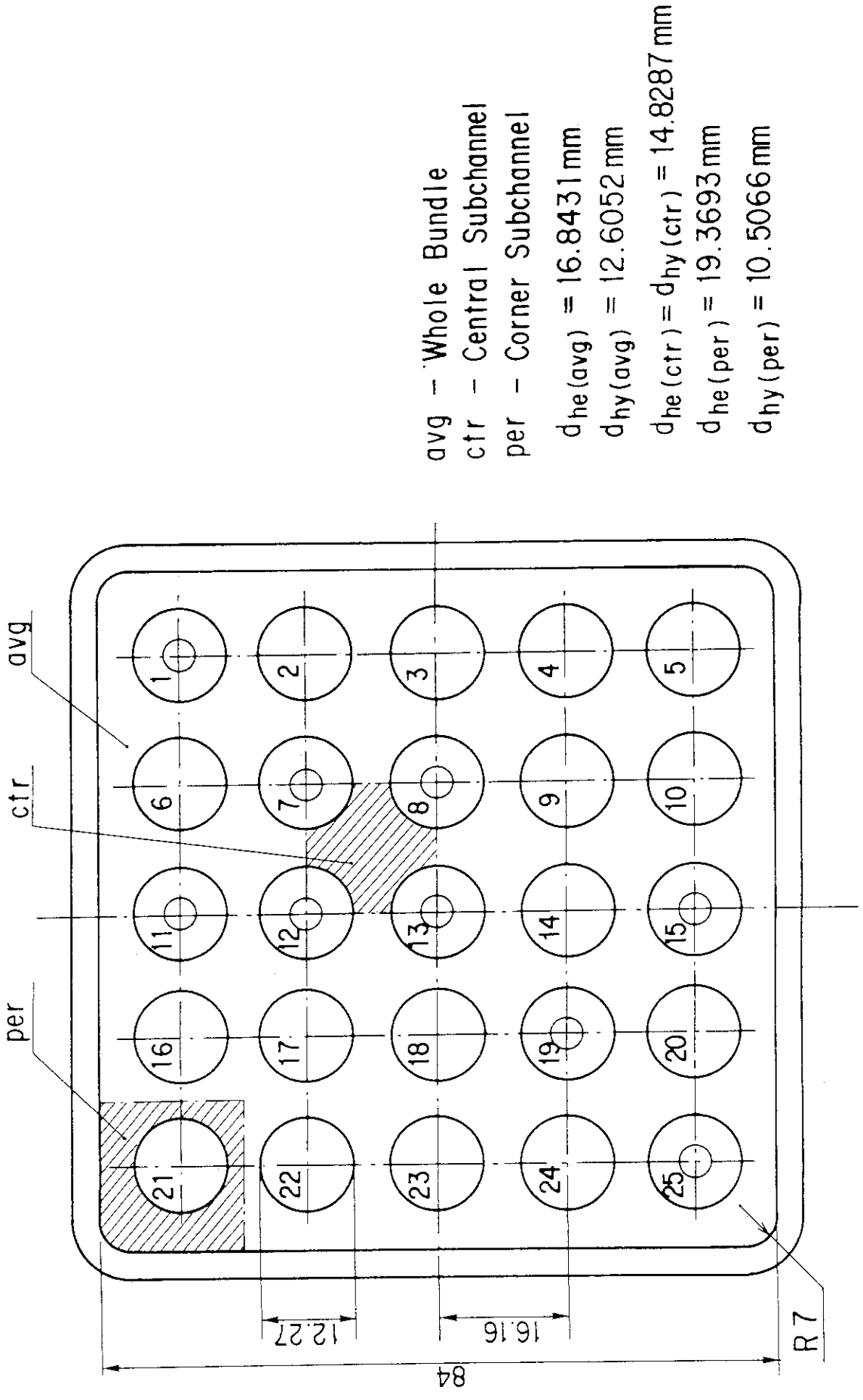

Fig. 5 Bundle cross section and pertinent dimensions

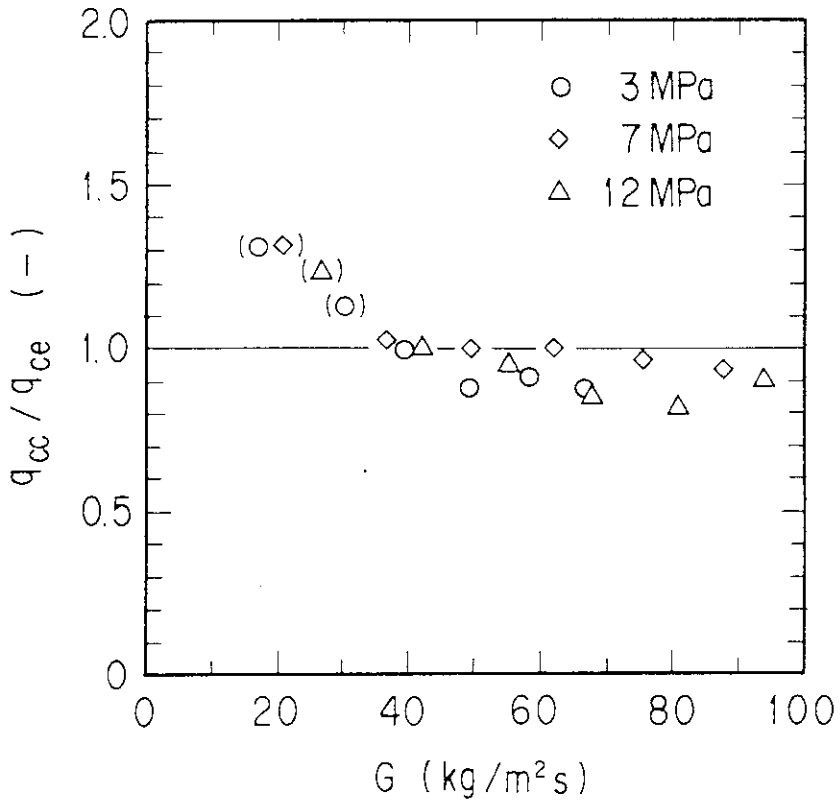

Fig. 6 Bowring correlation performance ($l_{do(ctr)}$, $d_{h(ctr)}$)

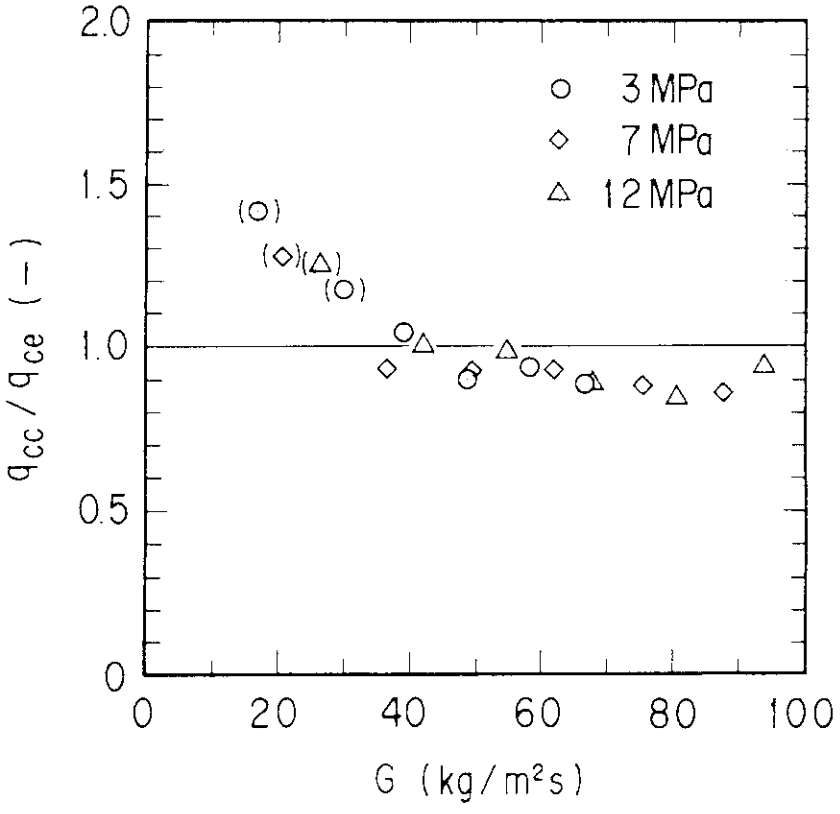

Fig. 7 Katto correlation performance ($l_{do(ctr)}$, $d_{h(ctr)}$)

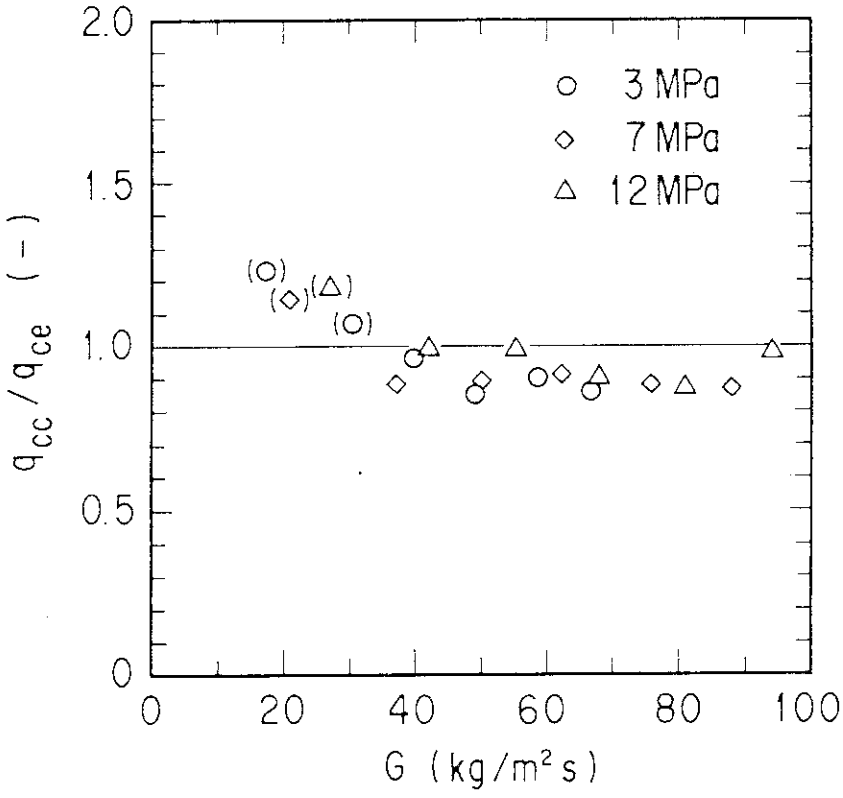

Fig. 8 V-equation performance ($l_{do(ctr)}$, $d_{h(ctr)}$)

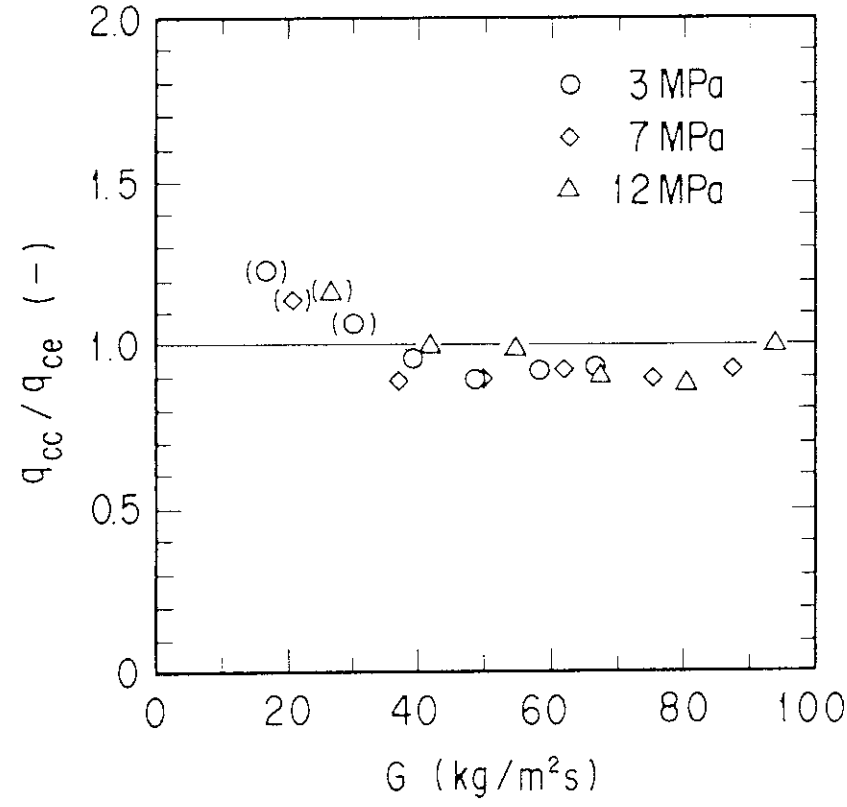

Fig. 9 V-equation performance ($l_{do(avg)}$, $d_{h(ctr)}$)

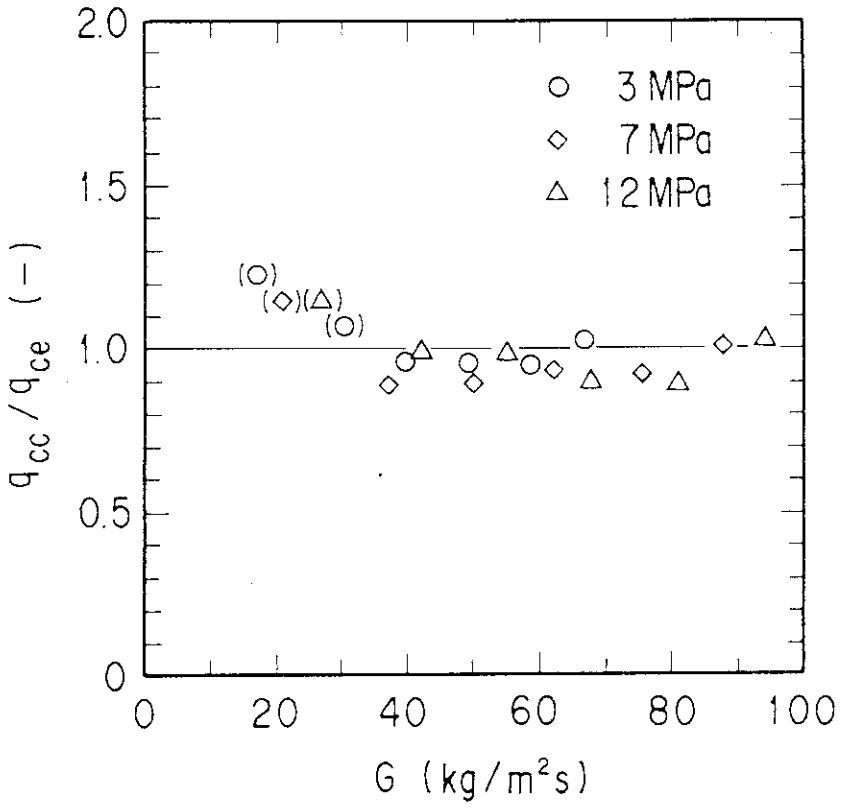

Fig. 10 V-equation performance ($l_{do(per)}$, $d_{h(ctr)}$)

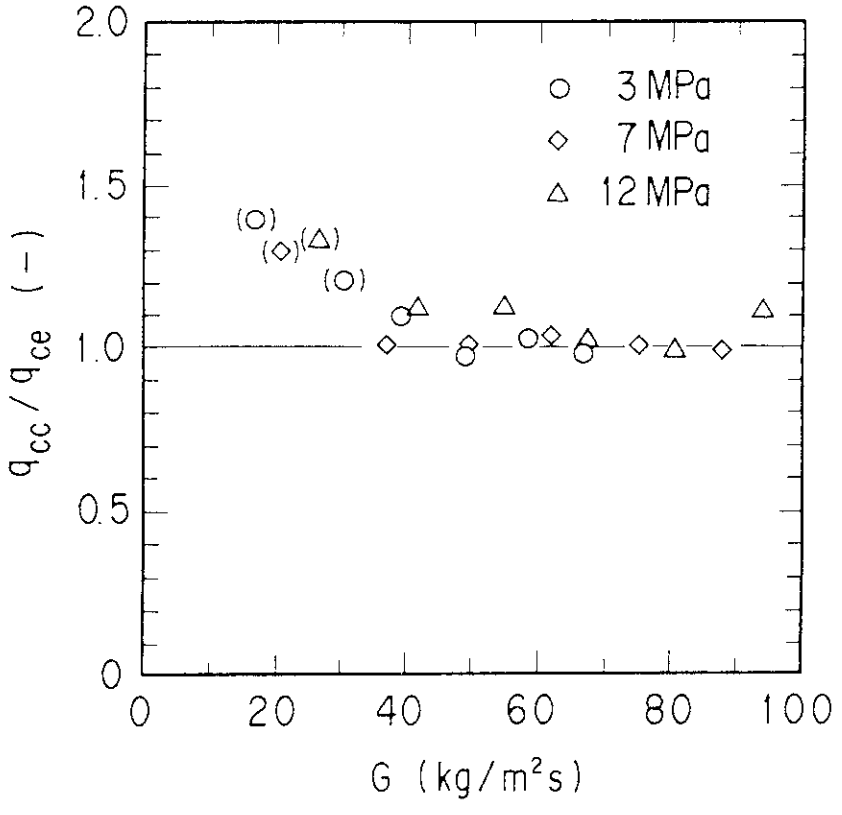

Fig. 11 V-equation performance ($l_{do(ctr)}$, $d_{h(avg)}$)

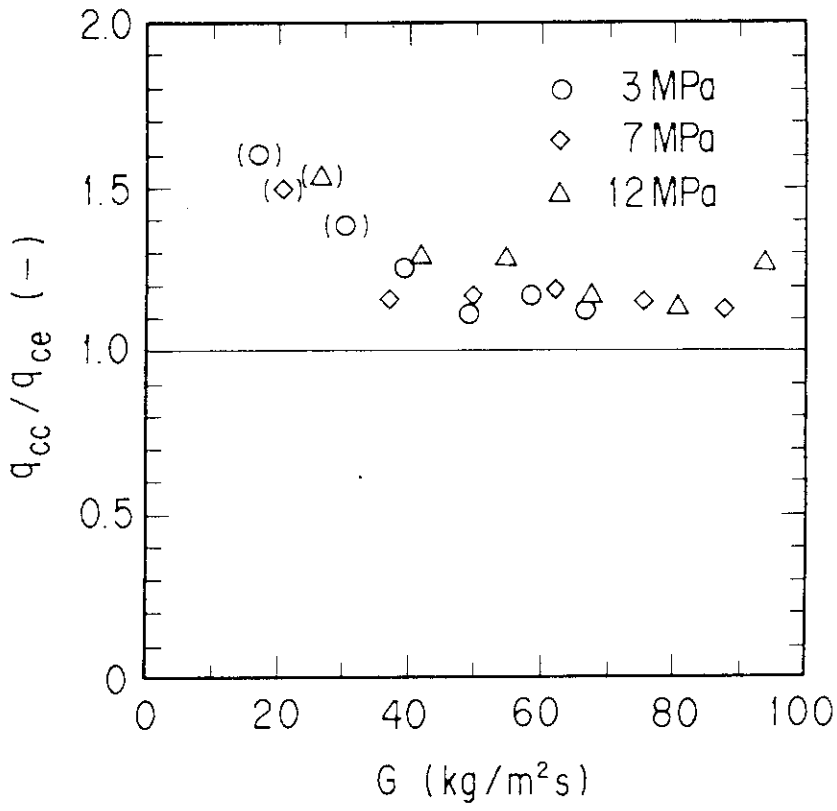

Fig. 12 V-equation performance ($l_{do(ctr)}$, $d_{h(per)}$)